Journal of Applied Polymer Science

Consolidation by Spark Plasma Sintering of Polyimide and Polyetheretherketone

Maxime Schwertz,[1,2] Sébastien Lemonnier,[1] Elodie Barraud,[1] Adele Carradò,[3] Marie-France Vallat,[2] Michel Nardin[2]

[1]French-German Research Institute of Saint-Louis, 5, rue du Général Cassagnou, 68300 Saint-Louis, France
[2]Institut de Science des Matériaux de Mulhouse UMR 7361 CNRS UHA, 15, rue Jean Starcky, 68057 Mulhouse, France
[3]Institut de Physique et Chimie des Matériaux de Strasbourg UMR 7504 CNRS UdS, 23, rue du Loess, 67034 Strasbourg, France
Correspondence to: M. Schwertz (E-mail: maxime.schwertz@isl.eu)

ABSTRACT: This article presents two high-temperature thermoplastic powders which were sintered by spark plasma sintering in order to get homogeneous mechanical properties. Dense polyimide (PI) and polyetheretherketone (PEEK) specimens were obtained at temperatures as low as 320°C for PI and 200°C for PEEK, respectively. Relative densities higher than 99% were reached for both materials. In order to characterize their properties, *in situ* measurements with compression and hardness tests were carried out on sintered samples. This method allowed to obtain polymeric materials with improved mechanical properties. © 2014 Wiley Periodicals, Inc. J. Appl. Polym. Sci. **2014**, *131*, 40783.

KEYWORDS: mechanical properties; spark plasma sintering; structure-property relations; thermoplastics

accepted 28 March 2014
DOI: 10.1002/app.40783

INTRODUCTION

For decades, high-performance thermoplastics have aroused considerable interest. In this class of polymers, polyimide (PI) and polyetheretherketone (PEEK) have been extensively investigated. Their success is largely due to the unique combination of thermo-oxidative stability with high wear resistance, stiffness, chemical and solvent resistance, a low dielectric constant, and a high mechanical strength.[1–4] They are widely used in high-temperature composites, adhesives, dielectrics, photoresists, nonlinear optical materials, and membrane materials, thus covering a large variety of fields of applications, such as aerospace, microelectronics, and automotive industries.[3,4]

However, these polymers cannot easily be processed by means of conventional polymer technologies such as injection moulding or extrusion as these methods require high temperatures, low viscosity, the complete melting of the polymer, and also restrict the use of fillers. Moreover, these polymers display low solubility in most common solvents at room temperature, except for strong protonating acids.

On account of the above-mentioned limitations, another method allowing the successful consolidation of polymers can be considered: powder metallurgy (P/M). Two major advantages of this approach are that higher pressures can be applied and fillers can be introduced more easily, compared with conventional polymer processing techniques. Compression moulding was applied to the consolidation of PEEK,[5] polytetrafluoroethylene (PTFE),[6,7] polyamides (PA),[8] and ultra-high molecular weight polyethylene (UHMWPE).[9] The strength of this method is that it increases the stiffness of the material by improving its crystalline organization or by introducing fibres. An alternative P/M process—called microwave sintering—was applied to add fillers (SiC particles) during the consolidation of PEEK-based coatings.[10] Moreover, a high-velocity compaction (HVC) technique was used for sintering polyoxymethylene (POM),[11] UHMWPE,[12] and PA;[13] indeed, it makes it possible to increase Young's modulus and the yield stress beyond conventional values by exerting higher pressures on the powder. Finally, selective laser sintering (SLS) was employed for the consolidation of PA[14] and PEEK[15] in order to obtain prototyping tools with complex geometries through computer-aided design (CAD). In addition, the process durations involved in the P/M method are time-saving, compared with the conventional ones: only a few minutes are necessary, instead of several hours.

Among the sintering processes, the recently widespread use of the spark plasma sintering (SPS) method has resulted in a considerable amount of literature and patents.[16,17] To our knowledge, very few studies based on the application of this

technique for the consolidation of polymers, more precisely high-temperature thermoplastics, have been published so far. Omori et al.[18,19] studied the consolidation of a thermosetting PI by SPS. According to the authors, the suitable consolidation temperature varied, depending on the applied pressure. PI was first partially carbonized at a temperature higher than 300°C at a pressure >19.6 MPa and then at a temperature higher than 230°C at 39.2 MPa. As PIs are heat-resistant polymers up to 400°C, the authors attributed this degradation to the energy of the plasma. According to them, the spark plasma energy should be low enough to damage the polymer structures, but high enough to excite certain chemical bonds, such as imide and ether groups. The latter should allow the formation of new chemical bonds resulting in cemented structures. Omori et al. observed that the mechanical properties were strongly dependent on the applied pressure. At 200°C, a pressure of 147 MPa was necessary to obtain a dense thermosetting PI sample with a maximum density of 1440 kg m^{-3} and as a result, a Young modulus of 4.40 GPa.

Tanaka et al.[20,21] employed PI-based composites made by SPS for friction and wear applications. They filled PI with carbon or diamond particles in order to enhance the wear properties of the composites. The pressure was set at 50 MPa and the composites were sintered at 220°C. At higher sintering temperatures, some cracks were observed and the antiwear properties deteriorated. In the same way, PI was used for the consolidation of reactive Ultem® powder-coated carbon fibre tow for space structure composites by resistive heating.[22] Rigid composites exhibiting voids and flaws were obtained. The authors ascribed these defects to non-optimized consolidation conditions.

The same weaknesses in the mechanical properties due to an early degradation (cracks, carbonization) were reported in previous studies based on PI/Cu and PI/Al functionally graded materials (FGMs).[23,24]

Therefore, the feasibility of using the SPS method to consolidate high-temperature thermoplastics was reported in the literature.[18–24] However, a poor mechanical strength was observed, due to a lack of optimization of the SPS process parameters. The principle of this process is that a pulsed electric current flows directly through a compaction die and a powder sample while uniaxial loading is applied in parallel. If the material is a conductive one, the electrical field heats both the die and the powder which is sintered by the Joule effect.[17,25] Nevertheless, if the powder is electrically insulating, only indirect heating by the die takes place. Recent studies combining simulations and experiments have shown that a significant temperature gradient, situated between the die and the sample as well as within the sample, can be observed during the SPS treatment.[26–32] This inhomogeneous distribution of temperature can occur in the case of insulating polymers or when the dimensions of the tools are not optimized.

Taking these problems into account, the purpose of this work is to study the sintering, by means of the SPS method, of fully dense high-temperature thermoplastics—PI and PEEK—exhibiting homogeneous mechanical properties in the bulk of the material under optimized sintering conditions. The temperature distribution and the homogeneity of the mechanical properties inside PI and PEEK were examined. In order to determine the characteristics of our materials, a dual approach was used. Firstly, the *in situ* temperatures were measured inside the sample to assess the temperature distribution. Secondly, the mechanical properties of the material were evaluated at three different locations in the sintered sample in order to verify the homogeneity inside the sample.

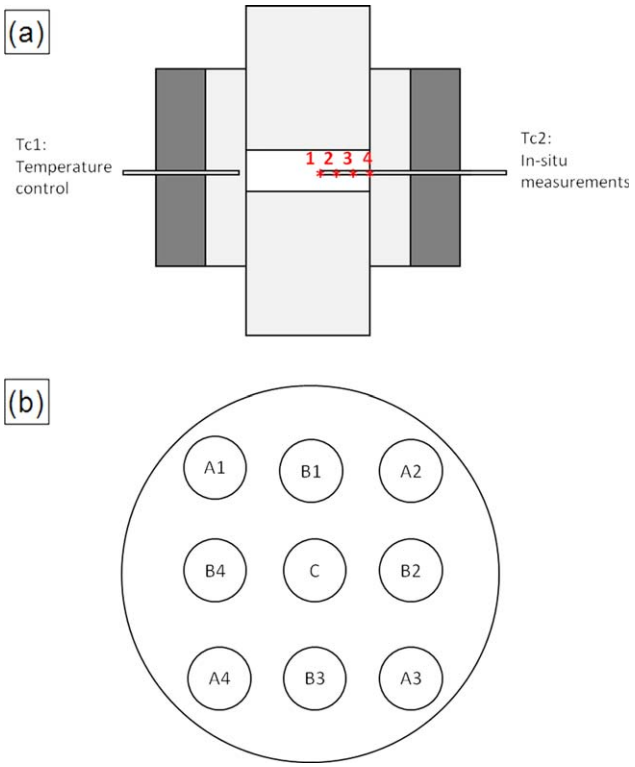

Figure 1. Sketches of (**a**) the specific tool designed for *in situ* measurements (locations 1 to 4 are explained in the text) and (**b**) the pellet with three different positions for mechanical characterization. [Color figure can be viewed in the online issue, which is available at wileyonlinelibrary.com.]

EXPERIMENTAL

High-Temperature Thermoplastics

An amorphous PI raw powder, supplied by Evonik, granulated into agglomerates ranging from 400 to 800 μm was used. The average particle size of the powder was in the range between 1 and 10 μm. The glass transition temperature (T_g) and the theoretical density were 320°C and 1380 kg m^{-3}, respectively.

A semi-crystalline PEEK powder, from Solvay, with particle sizes in the range between 20 and 140 μm was also considered. T_g and the melting temperature were equal to 150°C and 340°C, respectively, and the density was of 1300 kg m^{-3}.

SPS

Samples were sintered by using an HP D 125 SPS facility from FCT Systeme GmbH (Rauenstein, Germany). The *in situ* measurements required the development of a modified die with two holes, the first one for the temperature regulation and the second one for the temperature measurements inside the sample,

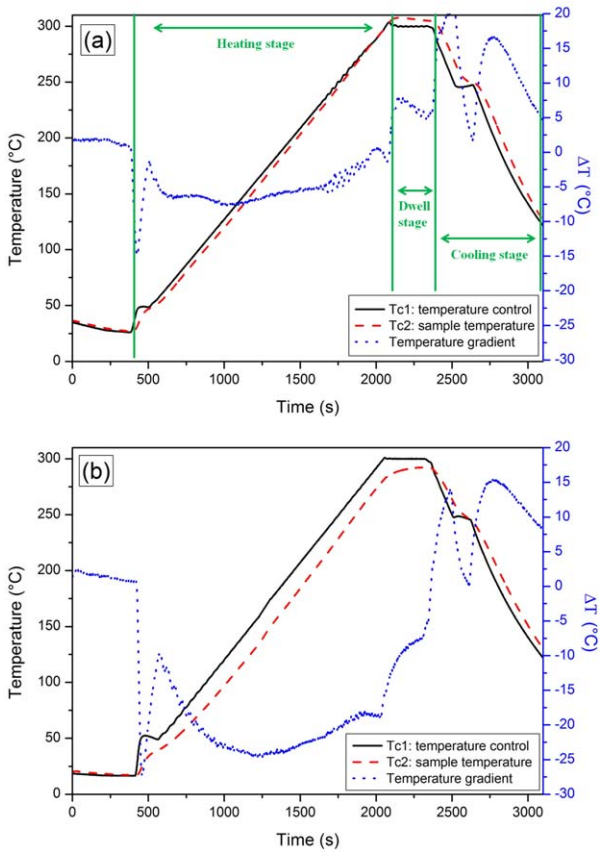

Figure 2. Temperature distribution inside the sintered (**a**) and powdery (**b**) PI samples measured *in situ* (point 1), during the sintering process. [Color figure can be viewed in the online issue, which is available at wileyonlinelibrary.com.]

as shown in Figure 1(a). Due to this additional hole bored through the die and on account of the mechanical limitations of graphite, this specific tool was made of steel. The powder was weighed so as to obtain 10-mm thick pellets with a diameter of 30 mm at maximum densification. The PI samples were heated with a rate of 10°C/min and consolidated at a pressure of 40 MPa and at a dwell time of 5 min.

Characterization

The densities of the sintered samples were determined by means of helium pycnometer method (Micromeritics AccuPyc 1330).

Shore D hardness (Innovatest THS-210) profile tests were performed according to the thickness and the diameter of the samples. The hardness values were measured each 5 mm.

Compression tests were carried out on specimens of 5 mm in diameter and thickness according to three positions in the sintered pellet [Figure 1(b), C = centre; B = borderline; A = angle]. This test is appropriated to evaluate the homogeneity inside the material as the final dimensions of the samples did not allow to perform tensile tests. The compression tests were executed with a testing machine (Instron 5500 K9400) at a crosshead displacement rate of 1 mm/min. Young's modulus, the compressive strength and the elongation at break were thus determined.

Table I. Shore D Hardness Profiles According to the Thickness (Line) and the Diameter (Column) Coordinates (mm) in the PI Sintered at 320°C

	5	10	15	20	25
0	83.6	86.8	87.6	86	83.2
5	88	87	87	87	88
10	85	87.4	88	87	85

After the compression tests, the fracture surfaces of the specimens were coated with an Au conductive layer and were observed in the compression axis by scanning electron microscopy (SEM, FEI Quanta 400).

RESULTS AND DISCUSSION

To evaluate the temperature distribution inside the sample, *in situ* temperature measurements were performed in PI on pellets which had been formerly sintered, as well as directly in the powder. The temperature control was ensured by the T_{c1} thermocouple and the measurements were recorded by the T_{c2} thermocouple as shown in Figure 1. The measurements within the samples were performed at four different distances from the inner wall of the die: 0 mm (sample/die interface: point 4), 5 mm (point 3), 10 mm (point 2), and 15 mm (centre: point 1). The temperature measured at the sample/die interface was used as a reference point for the calculation of the temperature gradient in the sample (ΔT). The maximum temperature was limited to 300°C so as to prevent the polymer from flowing out of the die, due to its low viscosity at a temperature close to T_g.

The measurements inside the samples show that the temperature gradient increases from the sample/die interface to the centre of the sample. As the temperature gradient is maximum in the centre, only the measurements performed at this location (point 1) are presented in Figure 2.

In both cases—powdery and sintered PIs—during the heating phase the temperature of the die (black curve, Figure 2) is higher than that of the sample (red dashed curve, Figure 2).

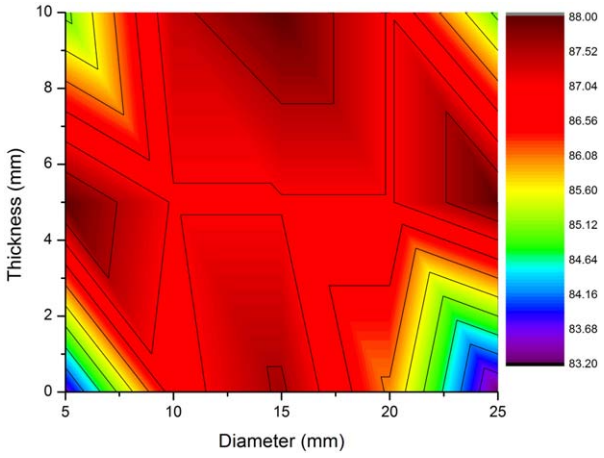

Figure 3. Hardness profile of a transversal cut of a PI sample sintered at 320°C. [Color figure can be viewed in the online issue, which is available at wileyonlinelibrary.com.]

Table II. Mechanical Properties of the Sintered PI Materials According to the Sintering Temperature

	PI sintered at 300°C			PI sintered at 320°C		
Positions	E (GPa)	σ_{max} (MPa)	ε_{max} (%)	E (GPa)	σ_{max} (MPa)	ε_{max} (%)
A1	2.69	201	20.9	3.14	773	63.4
A2	2.58	557	57.2	3.21	687	57.9
A3	3.20	536	53.8	3.16	649	59.6
A4	2.88	341	44.5	3.20	668	58.7
B1	2.34	600	56.0	3.17	724	59.1
B2	2.84	260	38.3	3.32	685	58.1
B3	2.86	491	53.0	3.23	675	59.4
B4	2.63	156	8.9	3.27	694	59.1
C	3.20	457	53.5	3.30	736	60.2

This effect is due to the samples being heated indirectly by the die. The temperature gradient ΔT (blue dotted curve, Figure 2) during this phase is estimated to be in the range between 20°C and 25°C. For the sintered sample, the temperature convergence occurs at the start of the dwell stage, whereas it takes place at the end of the dwell phase for the powder. The temperatures measured within the sample during the dwell phase are close to the temperature control recorded within the die. The desired temperatures are obtained with a temperature gradient from 5°C to 10°C. After the temperature convergence, inertia is observed, due to the thermal conductivity of the steel tools. The temperatures inside the sample are higher than those of the die.

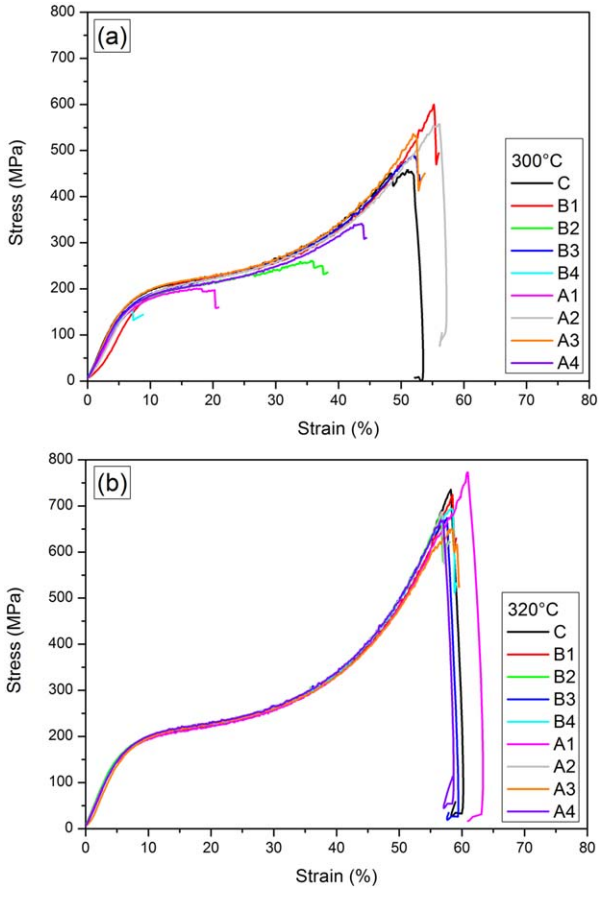

Figure 4. Compression curves for pellets sintered at 300°C (**a**) and 320°C (**b**) according to their positions inside the sample. [Color figure can be viewed in the online issue, which is available at wileyonlinelibrary.com.]

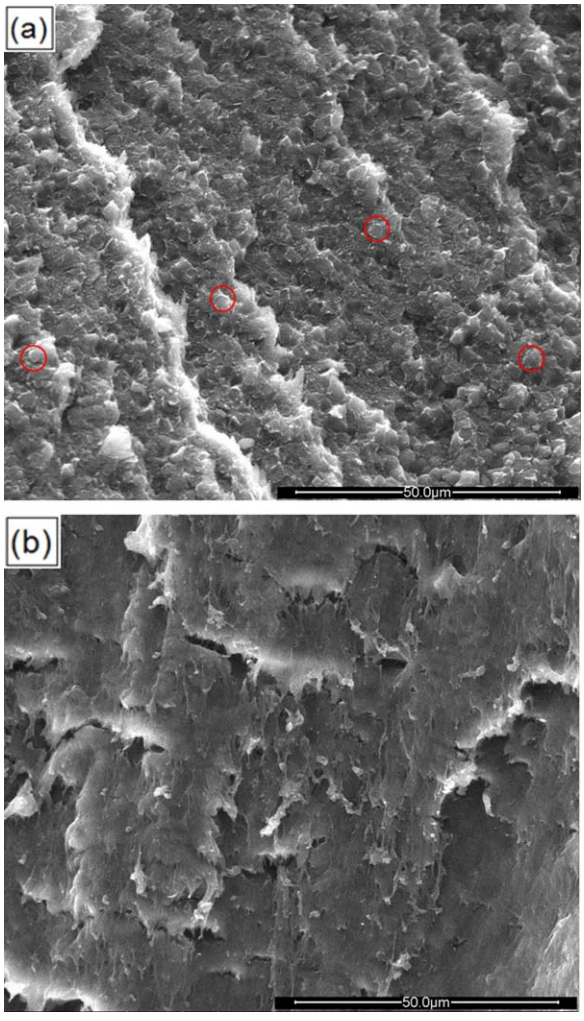

Figure 5. SEM images of PI sintered at 300°C with the presence of initial particles represented by *red circles* (**a**) and 320°C (**b**). [Color figure can be viewed in the online issue, which is available at wileyonlinelibrary.com.]

Table III. Mechanical Properties of the Sintered Polymers

	E (GPa)	σ_{max} (MPa)	ε_{max} (%)
PI	3.25 ± 0.05	707 ± 27	59.7 ± 0.7
PEEK	3.01 ± 0.08	144 ± 5	31.4 ± 1.7

This temperature gradient is more pronounced for the sintered sample. The measurements confirm that the temperature gradient is limited, due to the dimensions of the die that are well adapted to reach homogeneous temperature distribution inside the sample.

In order to estimate the influence of the temperature distribution on the bulk properties, density measurements combined with mechanical tests (Shore D hardness and compression tests) were performed. The PI samples were consolidated at a pressure of 40 MPa and at a dwell time of 5 min to ensure the temperature convergence and the homogeneity of the sample. The PI samples were first sintered at 300°C and then at 320°C. Relative densities higher than 99% were achieved.

The Shore D hardness values are homogeneous throughout the sample sintered at 320°C, as shown in Table I, except for the positions at the edges due to the stress distribution inside the sample under the uniaxial load conditions. This effect might be reduced by increasing the dwell time and the pressure. A transversal cut of a PI sample was represented in the Figure 3.

Compression tests were carried out on PI specimens at three different positions (A, B, C) in the sintered sample in order to compare the values of Young's modulus, of the compression at break and of the compressive strength, which were summarized in Table II according to the sintering temperature, 300°C or 320°C.

The compression curves reported in Figure 4 show the influence of the dwell temperature on the bulk properties.

The compression test curves are used for determining the homogeneity of the mechanical properties throughout the PI sample. At 300°C [Figure 4(a)], only the B4 specimen breaks in the elastic zone. The failure of the other specimens is observed either in the plastic zone (A1, B2, and A4) or in the viscoplastic one (C, B1, B3, A2, and A3). The latter five positions display a maximum compression at break as well as a maximum compressive strength. These properties are highly heterogeneous and strongly dependent on the positions selected. At the temperature of 300°C homogeneous mechanical properties cannot be obtained in the sample. By contrast, for the samples sintered at 320°C [Figure 4(b)], the compression curves appear to be very reproducible. The latter specimens break in the viscoplastic zone, at a compressive stress of about 700 MPa, corresponding to a compression ratio of approximately 60%.

The fracture surfaces were observed by SEM (Figure 5) after the compression tests in order to compare the structure of the fractured polymer with its mechanical properties. The micrographs of the sample sintered at 300°C [Figure 5(a)] show that the initial structure of the powder is still apparent with particle sizes in the range between 1 and 10 μm (some examples represented by red circles). The two SEM micrographs display the stratification of the polymer upon breakage, perpendicular to the compression axis. The type of fracture of the PI material sintered at 300°C seems to be fragile. By contrast, the PI sample sintered at 320°C reveals a more ductile fracture with the presence of fibrils and stretched particles. Grain boundaries are observed in the two PI specimens but are particularly visible in the case of the specimen sintered at 300°C. In fact, the particle boundaries are more pronounced at 300°C, whereas the structure for the PI obtained at 320°C looks smoother. At 320°C, the mobility of polymer chains is higher than at 300°C as the temperature is very close to T_g. It leads to a better inter-diffusion of the macromolecular chains at the interface of the particles and results in a better cohesion between the particles. These observations are consistent with the compression test results which show that the PI consolidated at 320°C exhibits the highest properties upon breakage.

The same approach allowing the evaluation of the mechanical properties was applied to the PEEK consolidation by means of the SPS method. This polymer was consolidated at 200°C and at 40 MPa with a dwell time of 5 min. The homogeneous mechanical properties of the PI and PEEK polymers are summarized in Table III.

CONCLUSIONS

Dense high-temperature PI and PEEK thermoplastic samples were obtained by means of the SPS method at 320°C and 200°C, respectively. The study of the temperature distribution and of the mechanical properties shows that the homogeneity inside the sample is achieved by increasing the sintering temperature so that it is equal to or higher than T_g. The compressive strength of PI approximately amounts to 700 MPa at a compression of 60%, which is the highest value reported in the literature.[1,3] The development of dense PEEK at a low temperature, for example, 200°C, with mechanical properties as effective as the standard ones is a new achievement.[33] These two materials may be considered in the transportation field as structural materials for light weighting applications.

ACKNOWLEDGMENTS

The authors thank the Direction Générale de l'Armement (DGA) for funding this research through the Ph.D. grant awarded to M. Schwertz.

REFERENCES

1. Sroog, C. E. *Prog. Polym. Sci.* **1991**, *16*, 561.
2. Attwood, T. E.; Dawson, P. C.; Freeman, J. L.; Hoy, L. R. J.; Roseand, J. B.; Staniland, P. A. *Polymer* **1981**, *22*, 1096.
3. Liaw, D.-J.; Wang, K.-L.; Huang, Y.-C.; Lee, K.-R.; Lai, J.-Y.; Ha, C.-S. *Prog. Polym. Sci.* **2012**, *37*, 907.
4. Díez-Pascual, A. M.; Naffakh, M.; Marco, C.; Ellisand, G.; Gómez-Fatou, M. A. *Prog. Mater. Sci.* **2012**, *57*, 1106.
5. Rellyand, J. J.; Kamel, L. *Polym. Eng. Sci.* **1989**, *29*, 1456.
6. Hambir, S. S.; Jogand, J. P.; Nadkarni, V. M. *Polym. Eng. Sci.* **1994**, *34*, 1065.

7. Zhaoand, Z. H.; Chen, J. N. *Compos. Part B-Eng.* **2011**, *42*, 1306.
8. Xingyuan, G.; Yucheng, L.; Wenhuiand, S.; Jingjiang, L. *Polym. J.* **2001**, *33*, 821.
9. Parasnisand, N. C.; Ramani, K. *J. Mater. Sci.-Mater. Med.* **1998**, *9*, 165.
10. Zhang, G.; Leparoux, S.; Liaoand, H.; Coddet, C. *Scr. Mater.* **2006**, *55*, 621.
11. Jauffres, D.; Lame, O.; Vigier, G.; Doreand, F.; Chervin, C. *J. Appl. Polym. Sci.* **2007**, *106*, 488.
12. Jauffres, D.; Lame, O.; Vigier, G.; Doreand, F.; Fridrici, V. *J. Appl. Polym. Sci.* **2008**, *110*, 2579.
13. Azhdar, B.; Stenbergand, B.; Kari, L. *Polym. Test.* **2006**, *25*, 114.
14. Goodridge, R. D.; Tuckand, C. J.; Hague, R. J. M. *Prog. Mater. Sci.* **2012**, *57*, 229.
15. Tan, K. H.; Chua, C. K.; Leong, K. F.; Cheah, C. M.; Cheang, P.; Abu Bakarand, M. S.; Cha, S. W. *Biomaterials* **2003**, *24*, 3115.
16. Grasso, S.; Sakkaand, Y.; Maizza, G. *Sci. Technol. Adv. Mater.* **2009**, *10*, 053001.
17. Munir, Z. A.; Quachand, D. V.; Ohyanagi, M. *J. Am. Ceram. Soc.* **2011**, *94*, 1.
18. Omori, M.; Okubo, A.; Gilhwanand, K.; Hirai, T. *J. Mater. Synth. Process.* **1997**, *5*, 279.
19. Omori, M. *Mater. Sci. Eng. A* **2000**, *287*, 183.
20. Tanaka, A.; Umeda, K.; Yudasaka, M.; Suzuki, M.; Ohana, T.; Yumuraand, M.; Iijima, S. *Tribol. Lett.* **2005**, *19*, 135.
21. Tanaka, A.; Umedaand, K.; Takatsu, S. *Wear* **2004**, *257*, 1096.
22. Naskarand, A. K.; Edie, D. D. *J. Compos. Mater.* **2006**, *40*, 1871.
23. Omori, M.; Okubo, A.; Kangand, G. H.; Hirai, T. In Functionally Graded Materials 1996; Ichiroand, S.; Yoshinari, M., Eds.; Elsevier Science B.V.: Amsterdam, **1997**; p 767.
24. Omori, M. 3rd International Symposium on Structural and Functional Gradient Materials, *Switzerland*, **1994**; p 667.
25. Orrù, R.; Licheri, R.; Locci, A. M.; Cincottiand, A.; Cao, G. *Mater. Sci. Eng. R: Rep.* **2009**, *63*, 127.
26. Anselmi-Tamburini, U.; Gennari, S.; Garayand, J. E.; Munir, Z. A. *Mater. Sci. Eng.* **2005**, *394*, 139.
27. Vanmeensel, K.; Laptev, A.; Hennicke, J.; Vleugelsand, J.; Van der Biest, O. *Acta Mater.* **2005**, *53*, 4379.
28. Wang, X.; Casolco, S. R.; Xuand, G.; Garay, J. E. *Acta Mater.* **2007**, *55*, 3611.
29. Molenat, G.; Durand, L.; Galyand, J.; Couret, A. *J. Metal.* **2010**, http://dx.doi.org/10.1155/2010/145431.
30. Allen, J. B.; Walter, C. *ISRN Mater. Sci.* **2012**, http://dx.doi.org/10.5402/2012/698158.
31. Olevsky, E. A.; Garcia-Cardona, C.; Bradbury, W. L.; Haines, C. D.; Martinand, D. G.; Kapoor, D. *J. Am. Ceram. Soc.* **2012**, *95*, 2414.
32. Voisin, T.; Durand, L.; Karnatak, N.; Le Gallet, S.; Thomas, M.; Le Berre, Y.; Castagnéand, J.-F.; Couret, A. *J. Mater. Process. Technol.* **2013**, *213*, 269.
33. Rae, P. J.; Brownand, E. N.; Orler, E. B. *Polymer* **2007**, *48*, 598.